Chinese Chemical Letters 31 (2020) 2941–2944

Contents lists available at ScienceDirect

Chinese Chemical Letters

journal homepage: www.elsevier.com/locate/cclet

Communication

A ratiometric near-infrared naphthalimide-based fluorescent probe with high sensitivity for detecting Fe^{2+} *in vivo*

Lina Huang[a], Yu Chen[a], Yuqiang Zhao[b], Yumin Wang[a], Junwei Xiong[a], Junfeng Zhang[a,*], Xianghua Wu[a,*], Ying Zhou[b,*]

[a] College of Chemistry and Chemical Engineering, Yunnan Normal University, Kunming 650500, China
[b] College of Chemical Science and Technology, Yunnan University, Kunming 650091, China

ARTICLE INFO

Article history:
Received 20 February 2020
Received in revised form 30 May 2020
Accepted 2 June 2020
Available online 4 June 2020

Keywords:
Fluorescent probe
Ratiometric
Fe^{2+}
Naphthalimide
Near-infrared

ABSTRACT

Iron is one of the essential trace elements in the human body. It plays an important role in human biology and pathology. Deregulation of iron levels in cells is associated with disease development. In this work, we synthesized a novel near-infrared intramolecular charge transfer (ICT) based ratiometric fluorescent probe to detect Fe^{2+}, by using naphthalimide and indole moieties as building blocks. Our work showed that the radiometric probe has excellent selectivity, sensitivity and rapid response. Moreover, we could successfully perform real-time monitoring of Fe^{2+} in HeLa cells and *C. elegans*.

As a vital element of life, iron can adopt multiple oxidation states, which makes it critical for catalytical conversion in biological systems. Its deregulation may trigger oxidative stress events, leading to dysregulation of iron levels and is associated with various aging-related diseases such as cardiovascular disease, neurodegenerative diseases, Alzheimer's disease and multiple cancers [1–5]. Iron binds to hemoglobin and promotes the oxygen transfer from the lungs to cells. At cellular level iron acts as part of cytochromes and respiratory enzymes to help electron transfer and participate in mitochondrial respiratory chain [6–8]. In many physiological processes, iron plays an indispensable role, mainly in the form of ferrous and iron ions. Therefore, it is of great interest to effectively monitor and detect ferrous ions.

Naphthalimide derivatives have gradually become one of the hot research subjects in the field of fluorescence probes, including pH probes [9–11], fluorescent probes for ions [12–15], biological small molecules [16–19] and macromolecules [20–23] probes, *etc*. In this study, we selected naphthalimide and indole as building blocks for a new ICT-based ratiometric fluorescence probe, based on the following considerations: (1) Naphthalimide dyes are classic intramolecular charge transfer (ICT) dyes, which have excellent two-photon characteristics. They are widely used to develop two-photon fluorescent probes [24–26]; (2) Due to the excited ICT state between the electron donor and the electron acceptor in the same dye molecule, the naphthalimide dye has a relatively large Stokes shift. This may be beneficial for probe design with long wavelengths, such as red or near-infrared emissions; (3) The indole moiety is a traditional structural unit of a cyanine derivative [27]. It is worth noting that due to the presence of the chemically active methylene of the indole unit, the structure of the innovative probe can be easily modified. In general, we combined the advantages of classic naphthalene dyes and traditional indole moieties to construct a near-infrared (NIR) ratiometric fluorescent probe **1** with a novel structure for detecting Fe^{2+}. From the structural perspective, probe **1** extends the π system by introducing naphthalene and indole moieties to achieve adjustable emission from visible spectrum to NIR and has a large red shift (Scheme 1).

Fluorescent probes have the advantages of low radioactivity, low cost, simplicity and rapid application [28–36]. In recent years, several fluorescent probes for detecting Fe^{3+} have been developed [37,38], but relatively few probes were developed for detecting Fe^{2+} [39–43]. Here we have developed a novel near-infrared ICT-based ratiometric fluorescence probe **1** to detect Fe^{2+}. Probe **1** was made up by two parts: One is the NIR fluorophore of naphthalimide

* Corresponding authors.
E-mail addresses: junfengzhang78@126.com (J. Zhang), chxhwu@sina.com (X. Wu), yingzhou@ynu.edu.cn (Y. Zhou).

https://doi.org/10.1016/j.cclet.2020.06.006
1001-8417/

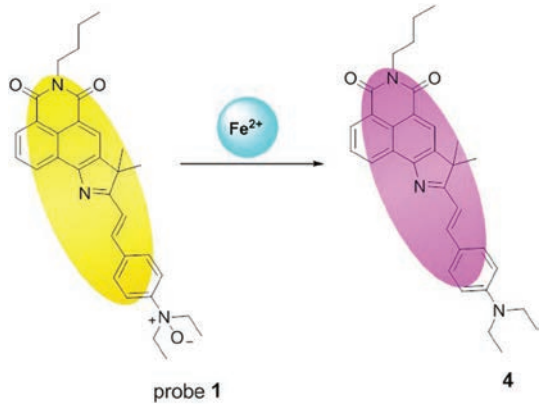

Scheme 1. The reaction mechanism of probe **1** with Fe^{2+}.

derivatives, the other is the Fe^{2+} detecting group of N-oxides. (Scheme S1 in Supporting information). Probe **1** showed fast response and a large red shift for Fe^{2+} detection. When the N-oxide was reduced by Fe^{2+}, the NIR fluorescence emission (λ_{em} = 690 nm) increased significantly with the increase of ICT. In addition, probe **1** exhibited high selectivity and sensitivity towards Fe^{2+} with low detection limit. Moreover, the novel probe **1** was successfully utilized for imaging Fe^{2+} in cells and *C. elegans*.

All chemicals and solvents were purchased from commercial suppliers, and were used directly without further purification in this article. Flash chromatography was carried out on silica gel (200–400 mesh), ^{1}H NMR and ^{13}C NMR spectra were recorded on Bruker 500 MHz and Bruker 126 MHz magnetic resonance spectrometers, respectively, mass spectrometry was recorded with Agilent 1100 LC-MSD/TOF mass spectrometer. The UV–vis spectra were recorded on UV-240 IPC spectrophotometer. The fluorescence spectra were recorded on F97XP FL spectrophotometer. The Olympus BX51 inverted fluorescence microscope and the Olympus IX71 inverted fluorescence microscope were used for biological imaging of cells and *C. elegans*, respectively. The fluorescence quantum yields were recorded with HORIBA Scientific Fluorolog.

Based on previous literatures [44,45], we synthesized intermediate compounds **1-4**. The structure of probe **1** was confirmed by ^{1}H NMR, ^{13}C NMR and HR-MS analysis. More details of synthetic processes and structure characterizations can be found in Supporting information.

To invest the responses of probe **1** towards Fe^{2+}, the spectral properties in PBS/DMSO = 2:8 (0.01 mol/L, pH 7.4) buffer solution were tested. We first investigate the UV–vis absorption of probe **1** to the addition of different equivalents of Fe^{2+}. As shown in Fig. 1a, the probe **1** solution showed an intensive peak at 420 nm. Upon the addition of Fe^{2+} (45 μmol/L), the absorption of probe **1** exhibited obvious decrease at 420 nm and strong increase at 510 nm. Then, the fluorescence spectra of probe **1** with different equivalents of Fe^{2+} were investigated. As proposed, free probe **1** (10 μmol/L) showed a fluorescence emission peak at 550 nm. With the addition of the Fe^{2+}, the intensity of probe **1** at 550 nm gradually decreased, while it enhanced at 690 nm, reaching the NIR region (Fig. 1b). It was observed that the color changed from yellow to pink. In PBS/DMSO = 2:8 (0.01 mol/L, pH 7.4) buffer solution with the probe **1** concentration of 2×10^{-6} mol/L, after adding different concentration of Fe^{2+}, the fluorescence intensity at 690 nm increased to a certain extent. The fluorescence intensity at 690 nm was excellent linearly associated with the concentration of Fe^{2+} (R^2 = 0.99287) (Fig. S1 in Supporting information). The calculated detection limit

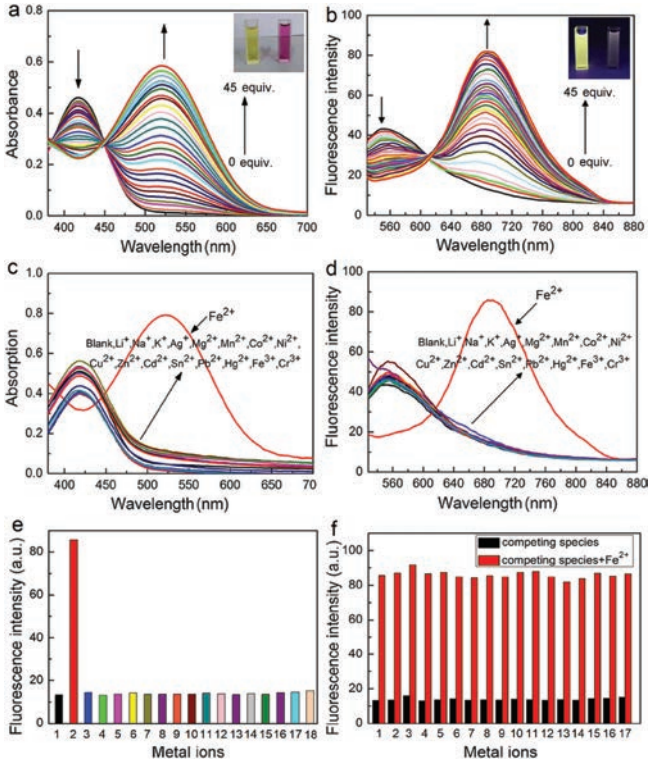

Fig. 1. The UV–vis absorption spectra (a) and fluorescence emission spectra (b) of probe **1** (2×10^{-5} mol/L) in the presence of Fe^{2+} (0-45 equiv.) in PBS/DMSO = 2:8 (0.01 mol/L, pH 7.4); (c) The UV–vis absorption spectra for probe **1** (2×10^{-5} mol/L) response to Fe^{2+} (45 equiv.) and other various metal ions (45 equiv.) in PBS/DMSO = 2:8 (0.01 mol/L, pH 7.4); (d) The fluorescence intensity of probe **1** (2×10^{-5} mol/L) response to Fe^{2+} (45 equiv.) and other various metal ions (45 equiv.) in PBS/DMSO = 2:8 (0.01 mol/L, pH 7.4); (e) The fluorescence intensity of probe **1** (2×10^{-5} mol/L) with different metal ions (45 equiv.) in PBS/DMSO = 2:8 (0.01 mol/L, pH 7.4) at 690 nm. From 1 to 18: Blank, Fe^{2+}, Na^+, K^+, Ag^+, Mg^{2+}, Mn^{2+}, Li^+, Co^{2+}, Ni^{2+}, Cu^{2+}, Zn^{2+}, Cd^{2+}, Sn^{2+}, Pb^{2+}, Hg^{2+}, Fe^{3+}, Cr^{3+}; (f) The fluorescence intensity variety of probe **1** (2×10^{-5} mol/L) towards Fe^{2+} (45 equiv.) with other various metal ions (45 equiv.) addition in PBS/DMSO = 2:8 (0.01 mol/L, pH 7.4) at 690 nm. λ_{ex} = 500 nm, slit: 10 nm. From 1 to 17: Blank, Li^+, Na^+, K^+, Ag^+, Mg^{2+}, Mn^{2+}, Co^{2+}, Ni^{2+}, Cu^{2+}, Zn^{2+}, Cd^{2+}, Sn^{2+}, Pb^{2+}, Hg^{2+}, Fe^{3+}, Cr^{3+}.

(LOD, 3σ/slope) of Fe^{2+} is 5.9 μmol/L, which also indicates a high sensitivity to Fe^{2+}.

Highly selective response is necessary for efficiently detecting relevant analytes among complex biological samples. Thus, we investigated the UV–vis absorption and fluorescence selectivity of probe **1** in PBS/DMSO = 2:8 (0.01 mol/L, pH 7.4) buffer solution. Upon treatment with various competitive species (Li^+, Na^+, K^+, Ag^+, Mg^{2+}, Mn^{2+}, Co^{2+}, Ni^{2+}, Cu^{2+}, Zn^{2+}, Cd^{2+}, Sn^{2+}, Pb^{2+}, Hg^{2+}, Fe^{3+}, Cr^{3+}, F^-, Cl^-, Br^-, NO_2^-, NO_3^-, SO_4^{2-}, SO_3^{2-}, HCO_3^-, ClO^-, AcO^-, Cys, Hcy, GSH), there was a strong absorption at 420 nm, which was consistent with the characteristic absorption of the free probe **1**. In addition, there was almost no obvious change. After the interaction of Fe^{2+} (45 μmol/L) with probe **1**, there was obvious absorption at 510 nm (Fig. 1c, Fig. S2 in Supporting information). The color of the probe **1** solution changed from yellow to pink. This result indicated that the probe **1** is an effective Fe^{2+} sensor, which can be visually addressed. Similarly, we tested the fluorescence spectrum selectivity of various analytes for probe **1**. As shown in Fig. 1d, after probe **1** interaction with Fe^{2+}, the emission peak changed significantly, and the maximum emission peak appeared at 690 nm. In contrast, when other analytes, such as common RSS, ROS and anions, were added to the solutions of probe **1**, the fluorescence spectrum hardly changed, which showed the newly

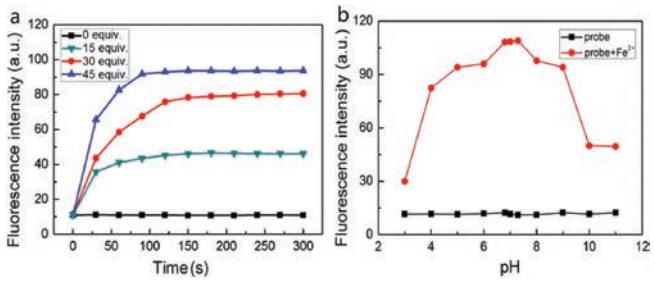

Fig. 2. (a) Fluorescence time response of probe **1** (2×10^{-5} mol/L) in the presence of different concentration of Fe^{2+} (0, 15, 30, 45 equiv.) in PBS/DMSO = 2:8 (0.01 mol/L, pH 7.4). (λ_{ex} = 500 nm, slit: 10 nm); (b) Fluorescence emission intensities (690 nm) of probe **1** (2×10^{-5} mol/L) at varied pH values (3-11) in the absence/presence of Fe^{2+} (45 equiv.).

developed probe **1** had an excellent selectivity in Fe^{2+} recognition (Fig. S3 in Supporting information). A histogram of the fluorescence intensity at the maximum emission of 690 nm is shown in Fig. 1e and Fig. S4 (Supporting information). More importantly, we also performed competition experiments. As shown in Fig. 1f and Fig. S5 (Supporting information), in the presence of other potentially interfering species, the fluorescence intensity of probe **1** at 690 nm response to Fe^{2+} in the presence of other potentially interfering species was approximately 5 times higher than that of the free probe **1**. The results showed that probe **1** has a high selectivity for Fe^{2+} even in a complex biological environment, and the specific fluorescence response of probe **1** towards Fe^{2+} was not affected by other biologically species analytes. In addition, the results confirming the probe **1** had great potential for the specific detection of Fe^{2+}.

It is worth noting that the fluorescence intensity increased at 690 nm in both different equivalent of Fe^{2+} (0, 15, 30, 45 equiv.) and time-dependent manner (Fig. 2a), and reached its maximum within 100 s. Furthermore, the fluorescence intensity of the free probe **1** remains almost unchanged for a long time. These results indicated that the reaction between probe **1** and Fe^{2+} is completed in a short time period, releasing the free compound **4** fluorophore. The presence of free compound **4** was verified by analyzing high-resolution mass spectrometry (HR-MS), and this mass peak is shown at *m/z* 493.2729. The proposed reaction mechanism shown in Scheme 1 was supported by these above experimental results.

In order to investigate the applicability of probe **1** in the physiological system *in vivo*, we evaluated the effect of probe **1** on Fe^{2+} in the range of pH 3−11. As shown in Fig. 2b, the fluorescence intensity of the free probe hardly changed at pH 3−11. After treatment with Fe^{2+}, a significant increase in fluorescence signal was observed over a wide pH range of 6–8, which indicates that probe **1** has the potential to detect Fe^{2+} under physiological conditions. The fluorescence quantum yields of probe **1** is 15.68% and after reaction with Fe^{2+} is 28.16%.

According to the reported literatures [46–48], Scheme 1 showed the potential response mechanism of the probe **1** to Fe^{2+}. Probe **1** was reduced to compound **4** with enhanced fluorescence from yellow to red. The products after the reaction between probe **1** and Fe^{2+} were analyzed by HR-MS. As can be seen from Fig. S6 (Supporting information), a new peak was found at *m/z* 494.2802, which corresponds to the reduced compound **4** (calculated value 493.2729). After the reaction between probe **1** and Fe^{2+} (45 equiv.) in PBS/DMSO = 2:8 (0.01 mol/L, pH 7.4) buffer solution, the fluorescence intensity at 690 nm (Fig. S7 in Supporting information) was similar to 45 equiv. compound **4** in PBS/DMSO = 2:8 (0.01 mol/L, pH 7.4) buffer solution. Therefore, the process of the Fe^{2+} detection of probe **1** was a typical ICT mechanism.

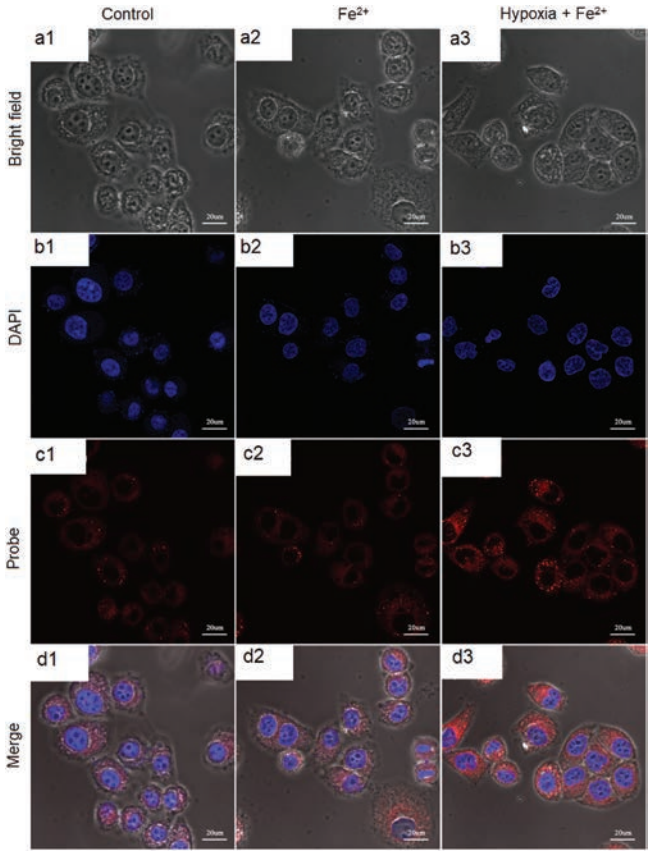

Fig. 3. Fluorescence confocal imaging of probe **1** (2×10^{-5} mol/L) in HeLa cells under normal oxygen and hypoxic conditions, incubated in the PBS buffer solutions at varying amount of Fe^{2+} for 2 h. (a1-d1): only with probe **1** (2×10^{-5} mol/L); (a2-d2): with probe **1** (2×10^{-5} mol/L) and Fe^{2+} (45 μmol/L); (a3-d3): with probe **1** (2×10^{-5} mol/L) and Fe^{2+} (45 μmol/L). (a1-a3): bright-field image; (b1-b3): blue channel, stained with DAPI; (c1-c3): red channel; (d1-d3): merged images. Scale bar: 20 μm.

To demonstrate the potential of probe **1** *in vivo*, probe **1** was used for fluorescence imaging studies in HeLa cells under hypoxia and normal oxygen conditions. In Fig. 3, HeLa cells were treated with different concentrations of Fe^{2+} (0, 15, 30 and 45 μmol/L) for 2 h, followed by incubation with probe **1** (20 μmol/L) at 37 °C for additional 2 h. No obvious change was observed only when HeLa cells were incubated with probe **1** (Fig. 3c1). When Fe^{2+} was added to the cells, the fluorescence intensity increased with increasing amounts of Fe^{2+}, and strong red fluorescence was observed throughout the cytoplasm. These results confirmed that probe **1** penetrates the living cell membrane and effectively detects Fe^{2+}.

Based on the fluorescence imaging performance of probe **1** in cells, we also completed the *in vivo* imaging study of probe **1** in *C. elegans*. As show in Fig. 4, the *C. elegans* were first treated with Fe^{2+} (45 μmol/L) for 2 h under the N_2 atmosphere and later treated with probe **1** for another 2 h at the room temperature (20 °C), a strong red fluorescence in emitting from the entire *C. elegans* body was observed. In contrast, *C. elegans* treated with probe **1** alone exhibited weaker fluorescence.

In summary, we have successfully designed and synthesized a near-infrared ratiometric fluorescent probe **1** for Fe^{2+} detection based on novel naphthalimide and indole derivatives as fluorophore. Probe **1** showed excellent Fe^{2+} sensing performance including predominant selectivity and sensitivity, low detection limit, rapid response, high stability over a wide pH range and large

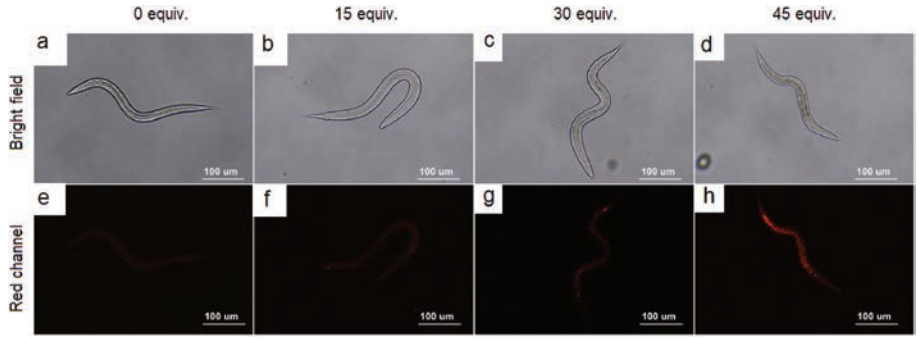

Fig. 4. Bright field images (a-d) and fluorescence images (e-h) in *C. elegans*. (a, e): probe **1** (2×10^{-5} mol/L) only; (b, f): probe **1** (2×10^{-5} mol/L) and Fe^{2+} (15 μmol/L); (c, g): probe **1** (2×10^{-5} mol/L) and Fe^{2+} (30 μmol/L); (d, h): probe **1** (2×10^{-5} mol/L) and Fe^{2+} (45 μmol/L). Fluorescence images were collected in red channels. Scale bar: 100 μm.

red shift. Notably, probe **1** was successfully employed to monitor Fe^{2+} in HeLa cells and *C. elegans*. Based on the above advantages of probe **1**, we believe that the probe **1** is a promising research tool for Fe^{2+} detection *in vitro* and *in vivo*.

Declaration of competing interest

The authors declare that they have no known competing financial interests or personal relationships that could have appeared to influence the work reported in this paper.

Acknowledgments

We thank the National Natural Science Foundation of China (Nos. 21672185 and 21867019) and the "Youth Talent of WanRen Project" Foundation of Yunnan Province of China for the financial support. J.F. Zhang acknowledges the "LianDa Scholar Project" and "Graduate Research and Innovation" Foundation of Yunnan Normal University (No. Ysdyjs2019122).

Appendix A. Supplementary data

Supplementary material related to this article can be found, in the online version, at doi:https://doi.org/10.1016/j.cclet.2020.06.006.

References

[1] S.A. James, B.R. Roberts, D.J. Hare, et al., Chem. Sci. 6 (2015) 2952–2962.
[2] S.V. Haehling, E.A. Jankowska, D.J. Veldhuisen, P. Ponikowski, S.D. Anker, Nat. Rev. Cardiol. 12 (2015) 659–669.
[3] D. Hare, S. Ayton, A. Bush, P.A. Lei, Front. Aging Neurosci. 5 (2013) 34.
[4] S.V. Torti, F.M. Torti, Nat. Rev. Cancer 13 (2013) 342–355.
[5] Z.K. Pinnix, L.D. Miller, W. Wang, Sci. Transl. Med. 2 (2010) 43–56.
[6] M.W. Hentze, M.U. Muckenthaler, B. Galy, C. Camaschella, Cell 142 (2010) 24–38.
[7] J. Wang, K. Pantopoulos, Biochem. J. 434 (2011) 365–381.
[8] D.C. Johnson, D.R. Dean, A.D. Smith, M.K. Johnson, Annu. Rev. Biochem. 74 (2005) 247–281.
[9] J. Xie, Y.H. Chen, W. Yang, et al., J. Photochem. Photobiol. A: Chem. 223 (2011) 111–118.
[10] V.B. Bojinov, D.B. Simeonov, N.I. Georgiev, Dye. Pigment. 76 (2008) 41–46.
[11] D.W. Cui, X.H. Qian, F.Y. Liu, R. Zhang, Org. Lett. 6 (2004) 2757–2760.
[12] A. Ajayaghosh, P. Carol, S. Sreejith, J. Am. Chem. Soc. 127 (2005) 14962–14963.
[13] S. Atilgan, T. Ozdemir, E.U. Akkaya, Org. Lett. 10 (2008) 4065–4067.
[14] J.H. Do, H.N. Kim, J.Y. Yoon, J.S. Kim, H.J. Kim, Org. Lett. 12 (2010) 932–934.
[15] I. Takashima, A. Kanegae, M. Sugimoto, et al., Inorg. Chem. 53 (2014) 7080–7082.
[16] J. Liu, Y.Q. Sun, Y.Y. Huo, et al., J. Am. Chem. Soc. 136 (2014) 574–577.
[17] L.W. He, Q.Y. Xu, Y. Liu, et al., ACS Appl. Mater. Interfaces 7 (2016) 12809–12813.
[18] L.F. Pang, Y.M. Zhou, W.L. Gao, et al., Ind. Eng. Chem. Res. 56 (2017) 7650–7655.
[19] X.Y. Zhu, Y. Li, W.Y. Zan, et al., Photochem. Photobiol. Sci. 15 (2016) 412–419.
[20] N. Pradhan, D. Jana, B.K. Ghorai, et al., ACS Appl. Mater. Interfaces 7 (2015) 25813–25820.
[21] Y. Kong, H.Q. Yao, H.J. Ren, et al., Proc. Natl. Acad. Sci. U. S. A. 107 (2010) 12239–12244.
[22] C.L. Teoh, D.D. Su, S. Sahu, et al., J. Am. Chem. Soc. 137 (2015) 13503–13509.
[23] Q. Jin, L. Feng, D.D. Wang, et al., ACS Appl. Mater. Interfaces 7 (2015) 28474–28481.
[24] H. Yu, Y. Xiao, L. Jin, J. Am. Chem. Soc. 134 (2012) 17486–17489.
[25] Z.R. Dai, G.B. Ge, L. Feng, J. Am. Chem. Soc. 137 (2015) 14488–14495.
[26] (a) M.H. Lee, H.M. Jeon, J.H. Han, et al., J. Am. Chem. Soc. 136 (2014) 8430–8437; (b) T. Guo, L. Cui, J. Shen, et al., Chem. Commun. (Camb.) 49 (2013) 1862–1864; (c) W. Xuan, R. Pan, Y. Wei, et al., Bioconjugate Chem. 27 (2016) 302–308.
[27] (a) X. Wu, B. Lin, M. Yu, et al., Chem. Sci. 6 (2015) 2002–2009; (b) Q.Q. Wan, S. Chen, W. Shi, L.H. Li, Angew. Chem. Int. Ed. 53 (2014) 10916; (c) S. Chen, Y. Hong, Y. Liu, et al., J. Am. Chem. Soc. 135 (2013) 4926–4929; (d) X. Jia, Q. Chen, Y. Yang, et al., J. Am. Chem. Soc. 138 (2016) 1065–1077.
[28] (a) X.M. Li, R.R. Zhao, Y. Yang, et al., Chin. Chem. Lett. 28 (2017) 1258–1261; (b) L. Yu, Y.M. Qiao, L.X. Miao, et al., Chin. Chem. Lett. 29 (2018) 1545–1559; (c) K.Y. Bi, R. Tan, R.T. Hao, et al., Chin. Chem. Lett. 30 (2019) 545–548; (d) Y. Chen, Y.Q. Zhao, P. Xie, et al., Dye. Pigment. 177 (2020) 108308.
[29] P. Ning, W. Wang, M. Chen, et al., Chin. Chem. Lett. 28 (2017) 1943–1951.
[30] L. Song, X.D. Sun, Y.H. Yao, et al., Chin. Chem. Lett. 27 (2016) 1776–1780.
[31] C. Duan, M. Won, P. Verwilst, et al., Anal. Chem. 91 (2019) 4172–4178.
[32] J.J. Wu, L.R. Jiang, P. Verwilst, et al., Chem. Commun. (Camb.) 55 (2019) 9947–9950.
[33] J.C. Xu, H.Q. Yuan, L.T. Zeng, G.M. Bao, Chin. Chem. Lett. 29 (2018) 1456–1464.
[34] W. Li, X.Y. Gong, X.P. Fan, et al., Chin. Chem. Lett. 30 (2019) 1775–1790.
[35] Q. Fang, L. Yang, H.Q. Xiong, et al., Chin. Chem. Lett. 31 (2020) 129–132.
[36] Q. Hu, C.Q. Qin, L. Huang, et al., Dye. Pigment. 149 (2018) 253–260.
[37] M.H. Lee, H. Lee, M.J. Chang, et al., Dye. Pigment. 130 (2016) 245–250.
[38] C. Wang, D. Zhang, X. Huang, et al., Talanta 128 (2014) 69–74.
[39] S. Maiti, Z. Aydin, Y. Zhang, M. Guo, Dalton Trans. 44 (2015) 8942–8949.
[40] T. Hirayama, H. Tsuboi, M. Niwa, et al., Chem. Sci. 8 (2017) 4858–4866.
[41] A.T. Aron, M.O. Loehr, J. Bogena, C.J. Chang, J. Am. Chem. Soc. 138 (2016) 14338–14346.
[42] G.G. Hou, C.H. Wang, J.F. Sun, et al., Biochem. Biophys. Res. Commun. 439 (2013) 459–463.
[43] X.P. Yang, Y.S. Wang, R. Liu, et al., Sens. Actuators B: Chem. 288 (2019) 217–224.
[44] H. Chen, Y.H. Tang, H.M. Shang, et al., J. Mater. Chem. B: Mater. Biol. Med. 5 (2017) 2436–2444.
[45] S. Zhou, Y.F. Rong, H. Wang, et al., Sens. Actuators B: Chem. 276 (2018) 136–141.
[46] Z. Mao, H. Jiang, Z. Li, et al., Chem. Sci. 8 (2017) 4533–4538.
[47] H. Li, Q. Yao, J. Fan, et al., Biosens. Bioelectron. 94 (2017) 536–543.
[48] T. Hirayama, K. Okuda, H. Nagasawa, Chem. Sci. 4 (2013) 1250.